11th International Symposium on Turbulence and Shear Flow Phenomena (TSFP11)
Southampton, UK, July 30 to August 2, 2019

A DIRECT NUMERICAL SIMULATION STUDY OF POLYMERS IN NEAR-WALL TURBULENCE

Junghoon Lee
Department of Computational Science and Engineering
Yonsei University
50 Yonsei-ro, Seodaemun-gu, Seoul 03722
j.h.lee@yonsei.ac.kr

Changhoon Lee
Department of Computational Science Engineering
Department of Mechanical Engineering
Yonsei University
50 Yonsei-ro, Seodaemun-gu, Seoul 03722
clee@yonsei.ac.kr

ABSTRACT

We investigated the dynamics of polymers in near-wall turbulence through a direct numerical simulation of turbulent channel flow, along with Brownian dynamics simulation. On average, polymer stretching is most pronounced in the streamwise direction at $y^+ \approx 10$. Consistent with the previous finding, our numerical results indicate that polymers are stretched in the streamwise direction as they travel in strong ejections. However, very strong stretching of polymers (i.e. with $|\vec{r}| > 0.9 r_{max}$) occurred mainly in strong sweeps than in strong ejections with no strong preferential orientation.

INTRODUCTION

It has been well known that in wall-bounded turbulence, a remarkable reduction of turbulent drag can occur due to a small amount of polymer molecules (Toms, 1948; White & Mungal, 2008). With this motivation, considerable attention has been paid to improving our understanding of how polymers interact with near-wall turbulence for several decades. Numerically, Lagrangian tracking of polymers using Brownian dynamics is a useful way of investigating their dynamics around coherent structures of near-wall turbulence. For example, Ilg *et al.* (2002) using a direct numerical simulation (DNS) of turbulent channel flow showed that polymers are highly stretched in the mean flow direction. Stone & Graham (2003) considered a model for the turbulent buffer layer and showed polymer stretching in the streamwise streaks and relaxation around streamwise vortices in the model flow. Terrapon *et al.* (2004) demonstrated that highly stretched polymers are found primarily in straining flows near the wall around streamwise vortices (i.e. ejections of low-speed fluid away from the wall) in a minimal channel. Bagheri *et al.* (2012) performed DNS of turbulent channel flow to show that polymers become more stretched and orient along the streamwise direction near the wall than in the core region.

In this study, we perform DNS of turbulent channel flow, along with Brownian dynamics simulation. We investigate the polymer dynamics around coherent flow structures of near-wall turbulence through conditional statistics of polymer elongation and orientation for various polymer time scales.

METHODOLOGY

Turbulent channel flow The governing equations for an incompressible channel flow are given by

$$\frac{D\vec{u}}{Dt} = -\frac{1}{\rho}\nabla p + \nu\nabla^2\vec{u}, \tag{1}$$

$$\nabla \cdot \vec{u} = 0, \tag{2}$$

where $\vec{u}$ and p indicate the fluid velocity vector and pressure, respectively, and ρ, ν are the fluid density and viscosity, respectively. A DNS was performed using the pseudo-spectral and Chebyshev-tau methods, without considering the effect of polymers on the fluid. The dealiased Fourier expansion in the homogeneous directions and the Chebyshev expansion in the wall-normal direction were used (Kim *et al.*, 1987). For time advancing, the viscous and nonlinear terms were discretized using the Crank–Nicolson and third-order three-stage Runge–Kutta schemes, respectively.

A Reynolds number of $Re_\tau = u_\tau \delta/\nu = 180$ was considered in this study, where u_τ and δ are the friction velocity and channel half width, respectively. In the streamwise (x), wall-normal (y) and spanwise directions (z), the domain size was $(4\pi\delta, 2\delta, 2\pi\delta)$ and the mesh was $(128, 129, 128)$. In the (x,z) directions, periodic boundary conditions were applied, and a no-slip condition was used at the walls.

Polymers The equation of motion for polymers can be established using a dumbbell model as (Watanabe

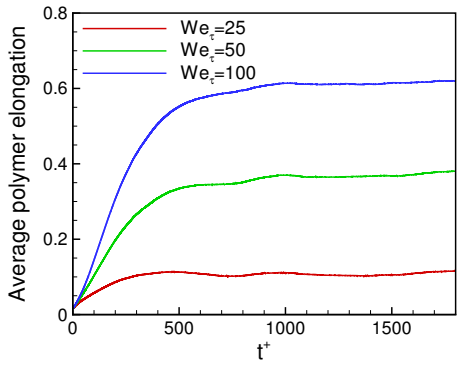

Figure 1. Temporal evolution of average polymer elongation $\langle|\vec{r}|\rangle/r_{max}$), averaged over all the polymers simulated.

& Gotoh, 2010),

$$\frac{d\vec{r}^{(m)}}{dt} = \vec{u}\left(\vec{q}_2^{(m)}(t),t\right) - \vec{u}\left(\vec{q}_1^{(m)}(t),t\right) + \frac{1}{\xi}\left(\vec{F}_2^{(m)} - \vec{F}_1^{(m)}\right) + \frac{1}{\xi}\left(\vec{W}_2^{(m)} - \vec{W}_1^{(m)}\right), \quad (3)$$

where $\vec{r}^{(m)}(=\vec{q}_2^{(m)} - \vec{q}_1^{(m)})$ represents the end-to-end distance vector of the m-th polymer, and $\xi = 6\pi\rho\nu a$ (a is the bead radius). $\vec{F}_n^{(m)}$ and $\vec{W}_n^{(m)}$ indicate the spring and Brownian forces, respectively, acting on the n-th bead for the m-th polymer. Here, the finitely extensible nonlinear elastic (FENE) effect was considered as,

$$\vec{F}_1^{(m)} = \gamma k\vec{r}^{(m)}, \quad \vec{F}_2^{(m)} = -\gamma k\vec{r}^{(m)}, \quad \gamma = \left[1 - \left(\frac{|\vec{r}^{(m)}|}{r_{max}}\right)^2\right]^{-1}, \quad (4)$$

where k is the spring constant and r_{max} is the maximum extension length of dumbbells. The characteristic time and length scales of polymers are defined, respectively, as

$$\tau_s = \frac{\xi}{4k}, \quad r_{eq} = \sqrt{\frac{\kappa_B T}{k}}, \quad (5)$$

where κ_B is the Boltzmann constant and T is temperature. Then, Weissenberg number is defined as

$$We_\tau = \frac{\tau_s u_\tau^2}{\nu}. \quad (6)$$

In this study, three different Weissenberg numbers of $We_\tau = 25, 50$ and 100 were considered for $r_{eq}^+ = 0.006$ and $r_{max}/r_{eq} = 100$. Note that hereinafter, the superscript plus sign $^+$ indicates normalization based on the wall units, u_τ and ν.

To calculate $\vec{u}$ at the bead position, the four-point Hermite interpolation scheme in the homogeneous directions and the fifth-order Lagrange polynomial interpolation scheme in the wall-normal direction were employed in this study. Time advancement for the polymer equation was performed using the third-order three-stage Runge-Kutta scheme. A time step of $\Delta t^+ = 0.054$ was used.

At $t = 0$, 100 000 polymers are randomly distributed in a fully developed channel flow field. Their initial length and orientation are given by $\vec{r}^{(m)}(t=0) = \sqrt{3}r_{eq}\vec{n}_r$, where $\vec{n}_r$ is the unit vector in the random direction (Watanabe & Gotoh, 2014). Note that the simulated polymers never touched the wall during the entire period of simulation, $0 < t^+ < 1800$. For polymers moving outside the computational domain in the (x,z) directions, periodic conditions were employed. The effect of inter-polymer interactions was not considered in this study.

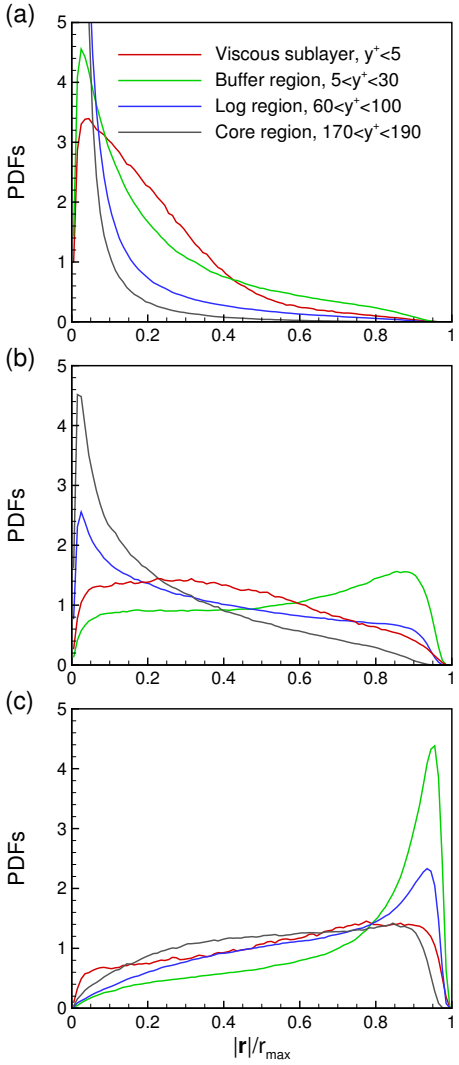

Figure 2. Probability density functions of $|\vec{r}|/r_{max}$ in the various regions of turbulent channel flow. (a) $We_\tau = 25$; (b) $We_\tau = 50$; (c) $We_\tau = 100$.

Figure 1 shows the temporal evolution of average polymer elongation $\langle|\vec{r}|\rangle/r_{max}$, where angle brackets $\langle\cdot\rangle$ indicate the ensemble-average over all the polymers simulated. In the figure, the averaged polymer elongation appears to reach steady state when $t^+ > 1000$. Therefore, in the following section our results were obtained only after $t^+ = 1000$.

RESULTS AND DISCUSSION

Figure 2 shows the probability density functions (PDFs) of $|\vec{r}|/r_{max}$ in the various regions of turbulent channel flow. For the smallest We_τ, the PDFs are highly skewed toward smaller values with their peaks at $|\vec{r}| < 0.1r_{max}$ in all the regions, indicating that polymers with $We_\tau = 25$ remain mostly coiled. However, for the largest We_τ, the opposite

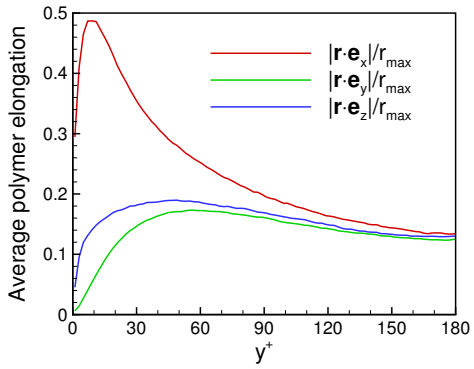

Figure 3. Wall-normal profiles of the mean values of $|\vec{r}\cdot\vec{e}_x|$, $|\vec{r}\cdot\vec{e}_y|$ and $|\vec{r}\cdot\vec{e}_z|$, averaged over the x,z directions, for $We_\tau = 50$.

is true, i.e. the PDFs become skewed toward higher values in all the regions. Note that in this case, the strongest peak of the PDFs is observed in the buffer region, indicating that polymers are most efficiently stretched there. This is also seen at the intermediate We_τ, for which the PDF is skewed toward $|\vec{r}| = r_{max}$ only in the buffer region.

Figure 3 displays the wall-normal profiles of the mean values of $|\vec{r}\cdot\vec{e}_x|$, $|\vec{r}\cdot\vec{e}_y|$ and $|\vec{r}\cdot\vec{e}_z|$, averaged over the x,z directions, for $We_\tau = 50$, where $\vec{e}_x, \vec{e}_y$ and $\vec{e}_z$ are the unit vectors in the x,y and z directions, respectively. It appears in the figure that the mean polymer elongation is most pronounced in the streamwise direction in the buffer layer. On the other hand, the mean polymer stretching in each direction becomes similar in the core region, indicating that polymer orientation exhibits no preferred direction on average.

In this study, we investigate the polymer dynamics in coherent sweeps ($u' > 0, v' < 0$) and ejections ($u' < 0, v' > 0$), generated by near-wall wall streamwise vortices, where u', v' are the fluctuating velocities in the x,y directions, respectively. Here, the condition that $|u'^+ v'^+| > 1$ in the region $5 < y^+ < 20$ (outside the viscous sublayer) was used to detect only strong sweeps and ejections. Figure 4 shows the PDFs of the elongation of polymers that travel in these two coherent flow regions. For the smallest We_τ, both the PDFs show peaks very close to $|\vec{r}| = 0$, consistent with figure 2, indicating a coiled state is most probable. As We_τ increases, very strong polymer stretching with $|\vec{r}| > 0.9 r_{max}$ occurs more commonly in strong sweeps than in strong ejections. On the other hand, in strong ejections, polymer stretching of $|\vec{r}| \approx 0.8 r_{max}$ is more probable.

In figure 5, the PDFs of the orientation of polymers in strong sweeps and ejections are shown for $We_\tau = 50$. Note that, the results for $We_\tau = 100$ are not shown in the figure, since there is no significant difference between the $We_\tau = 50$ and $We_\tau = 100$ cases. In strong ejections, polymers are strongly aligned along the streamwise direction, consistent with previous numerical results (Terrapon *et al.*, 2004), but such tendency, in particular the streamwise alignment in the (x,z) plane, is substantially reduced in strong sweeps.

Figure 6 illustrates the instantaneous snapshot of elongation and orientation of polymers with $We_\tau = 50$ at the buffer layer, along with the streamwise high- and low-speed fluid in the (x,z) plane. It appears in the figure that polymers are highly stretched in the buffer layer. In particular, the plotted polymer length becomes almost $|\vec{r}| \approx r_{max}$ in high-speed regions (associated with the sweep events). In high-speed regions, the almost fully stretched polymers exhibit no strong preferential orientation. On the other hand, in low-speed streaks (associated with the ejection events), polymers are preferentially aligned with the streamwise direction.

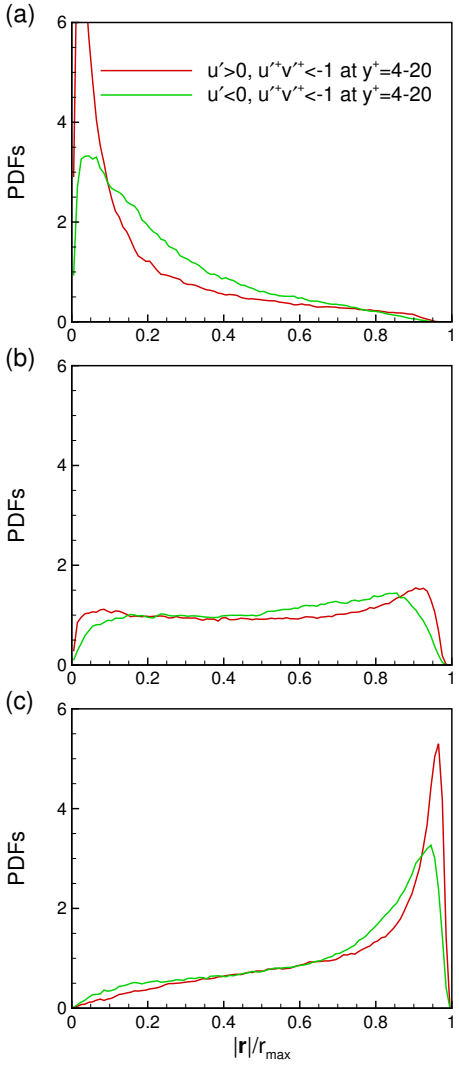

Figure 4. Probability density functions of polymer elongation in coherent flow patterns. (a) $We_\tau = 25$; (b) $We_\tau = 50$; (c) $We_\tau = 100$.

CONCLUDING REMARKS

In this study, we performed DNS of turbulent channel flow, along with Brownian dynamics simulation to investigate the polymer dynamics in near-wall turbulence. Our numerical results indicated that polymers are elongated in the mean flow direction in strong ejections, but very strong stretching of polymers (i.e. with $|\vec{r}| > 0.9 r_{max}$) occurs more commonly in strong sweeps than in strong ejections. In high-speed regions associated with the sweep events, the highly stretched polymers exhibited no strong preferential orientation. On average, polymer stretching was most pronounced in the streamwise direction at $y^+ \approx 10$.

ACKNOWLEDGMENT

This research was partially supported by the Graduate School of YONSEI University Research Scholarship Grants in 2017.

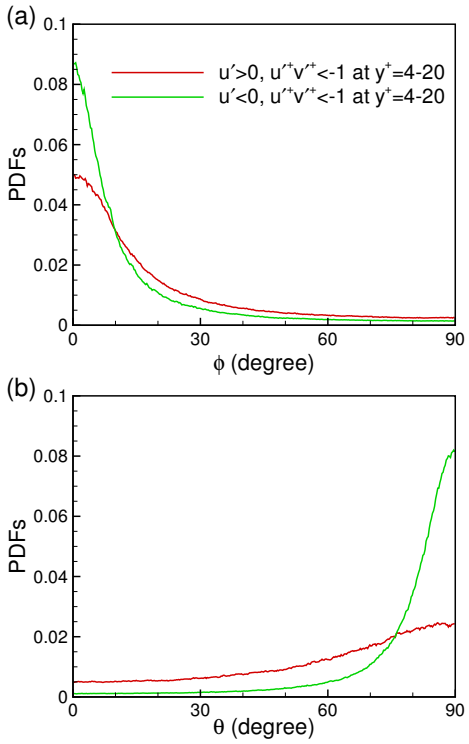

Figure 5. Probability density functions of polymer orientation in coherent flow patterns for $We_\tau = 50$. ϕ indicates the acute angle between $\vec{r}$ projected on the (x,y) planes and $\vec{e}_x$, and θ is the acute angle between $\vec{r}$ projected on the (x,z) plane and $\vec{e}_z$.

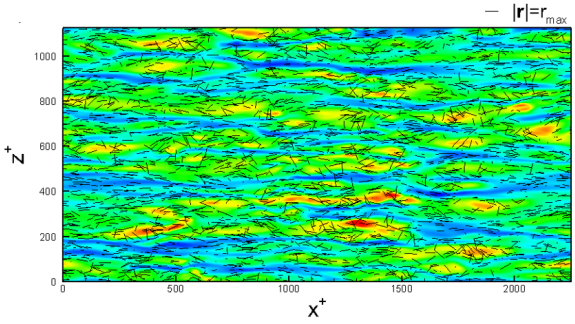

Figure 6. Instantaneous snapshot of polymer elongation and orientation for $We_\tau = 50$, along with high- and low-speed fluid regions (indicated by red and blue colors, respectively) in the (x,z) plane at $y^+ = 4-12$. For visualization purpose, 250 000 dumbbells were tracked here, and the length of polymers was drawn in an exaggerated scale (in fact, the maximum polymer length does not exceed 0.6 in wall units).

REFERENCES

Bagheri, F., Mitra, D., Perlekar, P. & Brandt, L. 2012 Statistics of polymer extensions in turbulent channel flow. *Physical Review E* **86**, 056314.

Ilg, P., De Angelis, E., Karlin, I. V., Casciola, C. M. & Succi, S. 2002 Polymer dynamics in wall turbulent flow. *Europhysics Letters* **58**, 616–622.

Kim, J., Moin, P. & Moser, R. 1987 Turbulence statistics in fully developed channel flow at low Reynolds number. *Journal of Fluid Mechanics* **177**, 133–166.

Stone, P. A. & Graham, M. D. 2003 Polymer dynamics in a model of the turbulent buffer layer. *Physics of Fluids* **15**, 1247–1256.

Terrapon, V. E., Dubief, Y., Moin, P., Shaqfeh, E. S. G. & Lele, S. K. 2004 Simulated polymer stretch in a turbulent flow using brownian dynamics. *Journal of Fluid Mechanics* **504**, 61–71.

Toms, B. A. 1948 Some observation on the flow of linear polymer solutions through straight tubes at large Reynolds number. In *Proceedings of the 1th International Congress on Rheology*, , vol. 2, pp. 135–141. North-Holland Amsterdam.

Watanabe, T. & Gotoh, T. 2010 Coil-stretch transition in an ensemble of polymers in isotropic turbulence. *Physical Review E* **81**, 066301.

Watanabe, T. & Gotoh, T. 2014 Power-law spectra formed by stretching polymers in decaying isotropic turbulence. *Physics of Fluids* **26**, 035110.

White, C. M. & Mungal, M. G. 2008 Mechanics and prediction of turbulent drag reduction with polymer additives. *Annual Review of Fluid Mechanics* **40**, 235–256.